Chapter 4: MATERIAL PROPERTIES AND LAB TEST PLAN

4.1 Introduction

A large-scale laboratory study was conducted to investigate the joint performance of the plain and fiber reinforced concretes through both the (i) B_{ALT} and (ii) S_{ALT} procedures. One PC and two FRC mixes were considered to evaluate the effect of the use of fibers has on joint performance. The relationship between LTE and number of load cycles (N) and cw were established for each concrete mixture. The majority of the testing consists of the $B_{ALT,}$ since it is more economical and faster than the S_{ALT}. This chapter presents the properties of the materials and the detailed plan for the laboratory study.

4.2 Materials

4.2.1 Aggregates and cement

In whitetopping, the material that plays the most significant role in joint performance is the coarse aggregates. Therefore, only one aggregate source was used throughout the study. River gravel conforming to AASHTO No. 57 gradation was used. The physical characteristics of the selected coarse aggregates are given in Table 4-1. The upper and lower limits of AASHTO No. 57 gradation and the actual gradation of the selected coarse aggregates are presented in Figure 4-1. One primary objective of this study is to investigate the contribution of fibers in joint performance. Therefore, an aggregate with a relatively high (34 percent) Los Angeles abrasion was selected so that the contribution of the fibers could be more prominently captured.

The fine aggregate used in casting all specimens is also from a single source. The fineness modulus, water absorption and saturated surface dry bulk specific gravity of the fine aggregate used are 2.86, 1.24 percent and 2.62, respectively. ASTM Type-I cement was used for casting all the specimens, except for a few trial specimens.

Table 4-1: Physical characteristics of the coarse aggregates.

Aggregate type	River gravel
Top size	1.0 inch
Gradation	AASHTO No. 57
Bulk specific gravity (SSD)	2.50
Water absorption capacity	2.07 %
Los Angeles abrasion value	34%

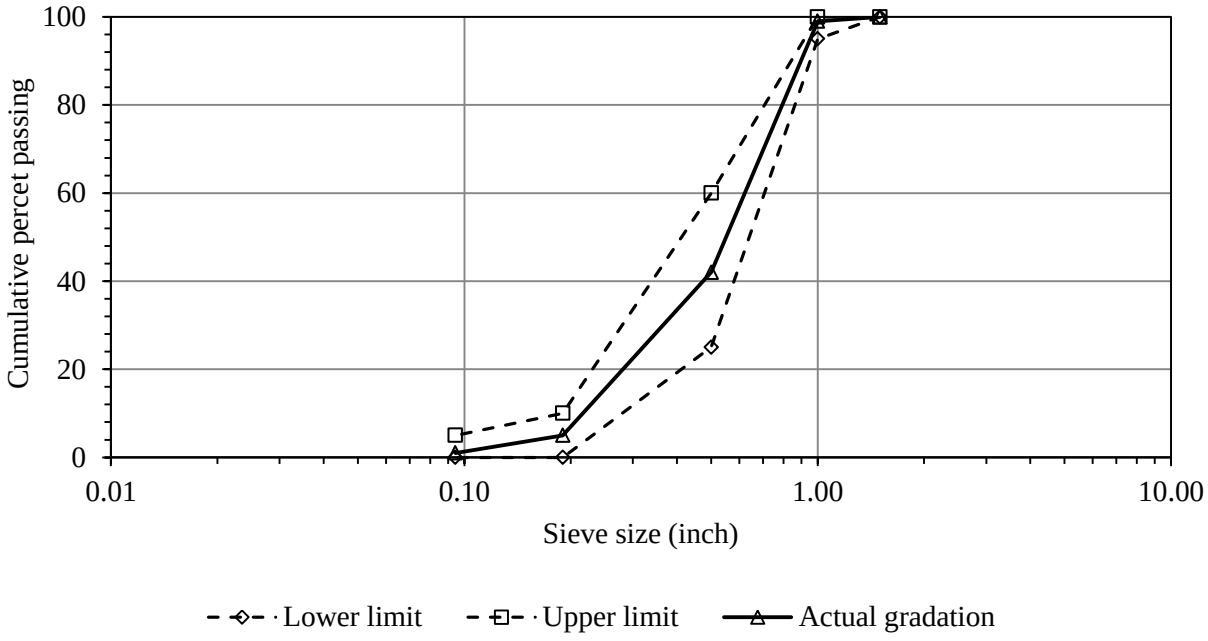

Figure 4-1: AASHTO No. 57 gradation and the actual gradation of the coarse aggregates used.

4.2.2 Fibers

A large variety of fibers are available with their primary differences being their raw material composition, shape, aspect ratio (AR) and stiffness. A review of the types of fibers commonly used in UTW was performed prior to the selection of the fibers to be included in this study (Barman, et al., 2010; Roesler, et al., 2008 and ACPA, 2009).

Types

A large number of whitetopping projects in the state of Illinois were constructed utilizing FRC. Some of those projects are summarized in Table 4-2. It can be seen that a large numbers of projects were constructed with structural synthetic fibers. In this project, straight synthetic (Figure 4-2a) and (ii) crimped synthetic (Figure 4-2b) structural fibers were selected. This point forward the first one is referred to as Fiber 1 or F1 and the second one as Fiber 2 or F2. The concrete mixes produced with F1 and F2 are referred to as FRC1 and FRC2, respectively. While F1 is the most frequently used synthetic structural fiber in whitetoppings constructed in the United States (ACPA, Illinois chapter, 2009), F2 provides the highest bond strength (Won, et al., 2006). Table 4-3 presents the features of the two selected fibers.

Table 4-2: Types of fibers used in whitetopping projects constructed in Illinois (ACPA, Illinois chapter, 2009).

Project location	Year of construction	Concrete layer thickness (in)	Slab size (ft x ft)	Fiber type	Dosage (lb/cy)
Stephenson county	1998	3	5.5 x 5.5	Synthetic	3
Mendota	1999	4.5	NA	Hybrid steel	50
Oak park	2001	4	5 x 6.5	structural steel	40
Peoria	2002	3	4 x 4	synthetic	3
Chicago/ cook co. Highway dept.	2003	4	3.5 x 4	structural synthetic	7.5
Schaumburg	2004	5	NA	structural synthetic	NA
Chicago, South Michigaan Ave.	2004	4	NA	structural synthetic	4

Kane county	2004	4.5	NA	structural synthetic	4
Cook county Highway	2004	4	NA	structural synthetic	7.5
Mundelein	2005	4	NA	structural synthetic	4
Olney	2008	3	4 x 4	synthetic	3
Macomb	2009	4	NA	structural synthetic	4
Logan County	2009	5.25	NA	structural synthetic	4
Henderson County	2010	5	NA	structural synthetic	4
Lombard	2010	4	4 x 4	structural synthetic	4
Shelby County	2010	4	NA	structural synthetic	4
Richland County	2010	5.5	5.5 x 5.5	structural synthetic	4
Clay County	2010	5.5	5.5 x 5.5	structural synthetic	4

Note: NA- Not available.

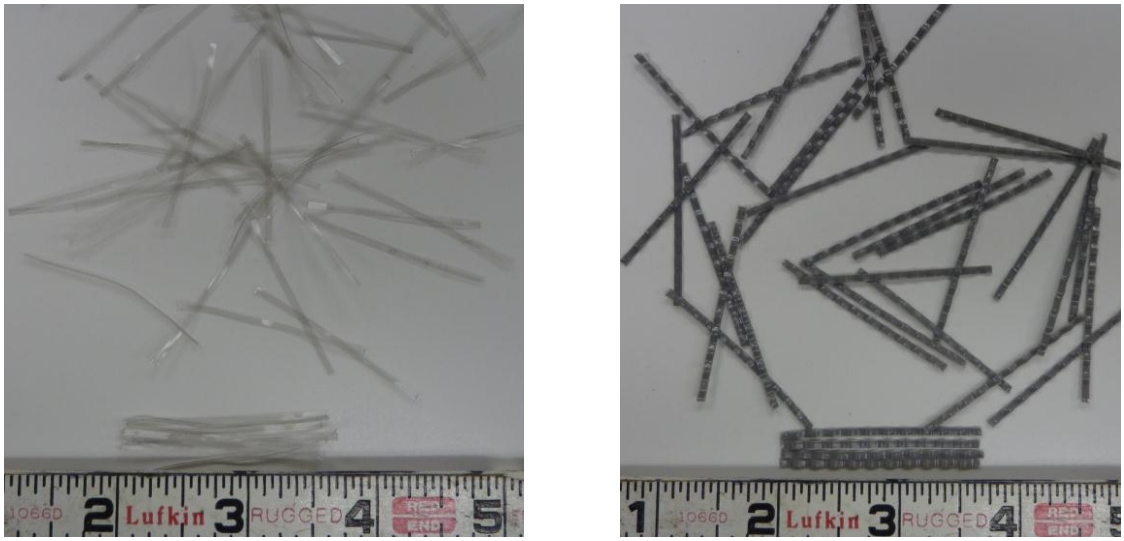

(a) **(b)**

Figure 4-2: Picture of the selected fibers (a) Straight synthetic-Strux: 90/40, (b) Crimped synthetic-Enduro 600.

Table 4-3: Features of the fibers selected for the present study.

Fiber category	Brand name	Length (in)	Shape	Cross section (in x in)	Specific gravity	Aspect ratio
Straight, synthetic	Strux: 90/40	1.57	Rectangular	0.05 x 0.004	0.92	90
Crimped, synthetic	Enduro 600	1.75	Rectangular	0.05 x 0.03	0.91	40

Volume fraction

The fiber volume fraction (V_f) may also play a significant role in the joint performance of whitetopping. However, at a given V_f, F1 and F2 may not necessarily provide an equal contribution to the joint performance due to their distinct features. Therefore, to select the most appropriate V_f for each selected fiber category, the literature was examined to investigate the influence of the shape and V_f on the strength of the concrete, especially on the residual strength ratio (RSR). Although FRC compared to the PC has several other benefits, RSR has been accounted for in one of the currently available whitetopping design procedures (Roesler, et al., 2008). This procedure proposed considering a 20 percent increase in the modulus of rupture (MOR) for a FRC with a RSR of 20 percent. The RSR for the concrete with different types of structural synthetic fibers were studied by Boredelon, 2005 and Roesler, et al., 2008.

Hannant, 1978, and Thomas & Ramaswamy, 2007 studied the strength contribution of the fibers through the combined influence of V_f and AR. In their studies, a new parameter, known as Reinforced Index (RI) was introduced. RI is expressed as below:

$$RI = V_f \times AR \tag{4-1}$$

Referring to this concept, the RSR test results from Boredelon, 2005 and Roesler, et al., 2008 were used to derive an approximation of the relationship between the RI and RSR, as shown in Figure 4-3. Three types of fibers are incorporated into this plot. A twisted synthetic fiber along with the straight and crimped synthetic fibers is also included. Only one test result is available for the concrete with crimped synthetic fibers. The RI for each fiber was computed using the information provided in the above two studies and from the manufacturer's datasheets. It can be seen that all three types of structural synthetic fibers follow a similar trend. The RSR increases with an increase in the RI. The RI corresponding to a 20% RSR was determined for each fiber

type using Figure 4-3. The corresponding V_f was then backed out using Equation 4-1. The dosage needed to obtain the V_f are provided in Table 4-4 for each fiber type.

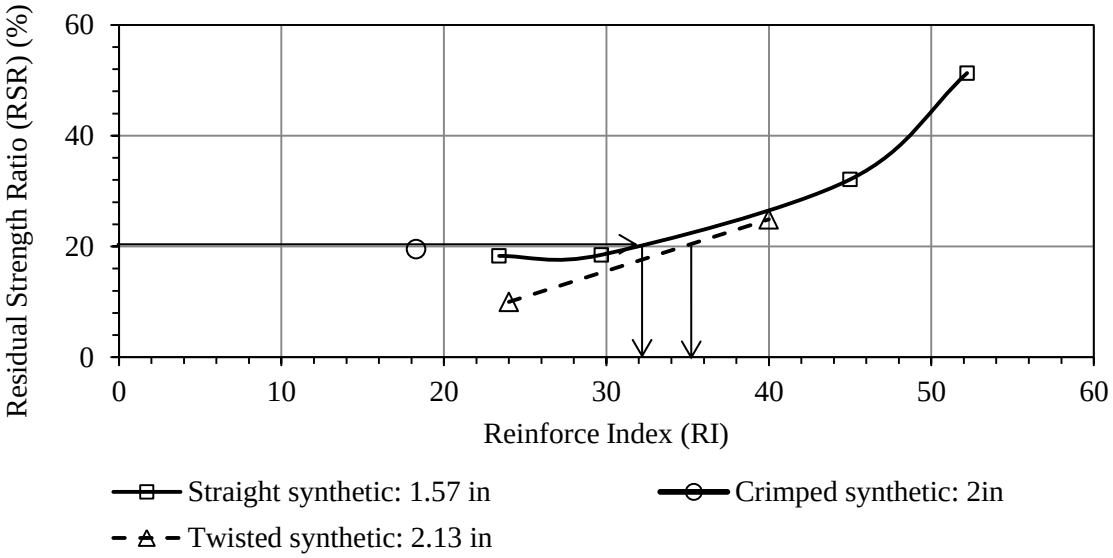

Figure 4-3: RI vs. RSR relationship for the structural synthetic FRC (After Boredelon, 2005 **and** Roesler, et al., 2008**).**

Table 4-4: Volume fraction and dosages of two selected fibers (After Boredelon, 2005 **and** Roesler, et al., 2008**).**

Straight synthetic. STRUX: 90/40		Crimped synthetic. Enduro 600	
Volume fraction (%)	Dosage (lb/cy)	Volume fraction (%)	Dosage (lb/cy)
0.36	5.25	0.43	6.20

4.2.3 Concrete Mixture Designs

The gravimetric and volumetric proportions for each concrete mixture are given in Table 4-5. The mixture designs were established based on typical mixes used for slip-form paving. A target water to cement ratio of 0.45 was used along with a target of 600 lbs of cement. A water reducer [CATEXOL 1000N (www.aximconcrete.com)] and air entrainer [CATEXOL AE 360 (www.aximconcrete.com)] were used to achieve the target slump of 2 ± 0.5 in and a 6 ± 1% air content.

Table 4-5: Target concrete mixture design.

Materials	Weight (lb/cy)	Volume (cft/cy)	Volume fraction
Coarse aggregates	1769	11.34	0.42
Fine aggregates	1089	6.66	0.25
Cement	600	3.05	0.11
Water	270	4.33	0.16
Air content	-	1.62	0.06
Water reducer, CATEXOL 1000N	0.75 oz/ 100 lb of cement		
Air entrainer, CATEXOL AE 360	1.5 oz/ 100 lb of cement		

In normal practice, when fiber is added into a mix, the volume of fine aggregates is reduced to accommodate the fiber for a given workability. However, the volume fraction of the fibers in the present study is only about 0.36 percent for F1 and 0.43 percent for F2, both of which are far lower than the target air content, and are in fact within the tolerance of the target air content. Therefore, the same mix proportion for the PC and FRC presented in Table 4-5 was adopted. The water reducer was increased to 1.5 oz per 100 lbs of cement in both F1 and F2 mixtures to maintain the desired level of workability.

4.3 Concrete Material Properties

The compressive strength, modulus of elasticity, RSR and MOR were measured at 28 days after casting. The MOR was also measured at 18 hours after casting. This coincides with the time at which the transverse cracks were initiated into the slabs and B_{ALT} beams. The VSTR for the B_{ALT} specimens was measured after fatiguing. A separate 6-in x 6-in x 24-in beam was also cast for each mixture for measuring the VSTR of crack face. Each of these separate beams were fractured for measuring VSTR at 18 hours using a procedure similar to that adopted for initiating crack in the B_{ALT} specimens. The VSTR was also measured for the slab crack face after the S_{ALT} was performed by cutting a section of the slab face from the transverse joint

The VSTR test was performed according to the procedure outlined in the Vandenbossche, 1999 study (Subsection 2.7.1). A photo of the equipment used for measuring the VSTR is provided in Figure 4-5. Using this equipment, the elevation of each grid from a datum surface is measured using a laser beam. A 5.5-in x 5.5-in area on the crack face of each B_{ALT} specimen was evaluated. The test procedure followed along with number of specimens tested for each mixture is summarized in Table 4-6.

Figure 4-4: Residual strength ratio testing.

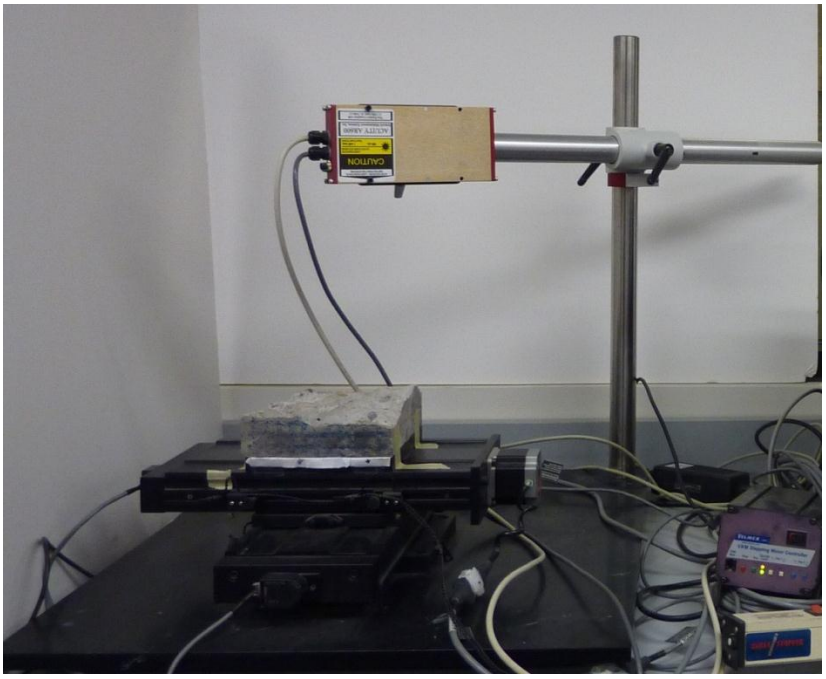

Figure 4-5: VSTR testing equipment.

Table 4-6: Test for characterizing concrete properties.

Test	Number of specimen	Age of specimen during testing	Specimen type/size	Test procedure reference
Compressive strength	6	28 days	Cylinder/ 6inch x 12 inch	ASTM-C39/C39M-12a, 2010
Modulus of elasticity	3	28 days	Cylinder/ 6inch x 12 inch	ASTM-C469/C469M, 2010
Modulus of rupture	6	18 hours	Beam/ 6 inch x 6 inch x 24 inch	ASTM-C78/C78M, 2010
	3	28 days		
Residual strength ratio	3	28 days	Beam/ 6 inch x 6 inch x 24 inch	ASTM-C1609/D1609M, 2010
VSTR of B_{ALT} specimen, before fatiguing	1	NA	Crack face of B_{ALT} specimen/ 5.5 inch x 6 inch	Vandenbossche, 1999
VSTR of B_{ALT} specimen, after fatiguing	4	NA	Crack face of B_{ALT} specimen/ 5.5 inch x 6 inch	Vandenbossche, 1999
VSTR of slab after fatiguing	3	NA	Crack face of slab joint/3.5 inch x 6 inch	Vandenbossche, 1999

4.4 Test Plan for the B_{ALT} Procedure

Before testing the three mixtures previously described, preliminary B_{ALT} was performed to establish the test protocol. This included establishing when and how data would be collected and what crack widths would be considered for fatiguing. Testing of the trial beams consisted of applying one million dynamic load cycles at a selected crack width to observe the fatiguing of the joint. Load and deflection profiles were recorded at different load cycles during the fatiguing process. After fatiguing, the crack width was opened in an approximately equal increment with the joint performance being evaluated to record the load and deflection profiles at various crack widths. After each crack width change, 995 load cycles (seating load cycles) were applied before collecting the load and deflection profiles for next five successive load cycles (total 1000 load cycles) to ensure the crack conditions at this crack width stabilized. Using the deflection profiles, LTE_B vs load cycles and LTE_B vs crack width relationships were determined for each trial beam to investigate the trends of drop in the LTE with increases in applied load cycles and crack width. These trends were used then used to plan the final test matrix.

Although at least 10 trials beams were tested, the joint performance results from two PC and two FRC1 beams are incorporated in this chapter. The LTE_B vs load cycles and LTE_B vs crack width for these beams are presented in Figure 4-6 through Figure 4-13. The two PC beams are labeled PT1 and PT2, whereas, the two FRC1 beams are labeled F1T1 and F1T2; P, T and F1 stand for PC, trial and FRC 1, respectively. It may be mentioned that the test results from the trial beams are not included in the final analysis, performed in Chapter 6. The test setup during testing of these beams was slightly different than the finalized fabrication. The trial beams were tested with a flat steel plate on top of the Fabcel layers instead of the top I-beam.

The first reported PC trial beam, PT1, was fatigued at a 0.023-in crack width. It was observed that the LTE_B under both the tension and compression loads remained relatively similar for the entire range of load cycles (Figure 4-6). Again, the LTE under the tension and compression loads are referred as $LTE_{B(t)}$ and $LTE_{B(c)}$, respectively. There is a slight increase in the LTE_B at around 500,000 load cycles, which might have been a measurement error. The average decrease in the LTE_B at the end of 1 million load cycles was 3 percent. After fatiguing, when the crack width was opened, LTE_B was found to be initially maintaining the same trend for up to a 0.043-in crack width, followed by a sharp decrease with any further increases in crack width (Figure 4-7).

The second reported PC trial beam, PT2, was fatigued at a 0.028-in crack width (Figure 4-8). It can be seen that the LTE_B did not decrease even after 1 million load cycles. LTE_B under both the tension and the compression load remains 90 percent throughout the entire range of load cycles. However, a sharp decrease in the LTE_B was observed when the crack width was opened after fatiguing of the joint (Figure 4-9). A variation between the $LTE_{B(t)}$ and $LTE_{B(c)}$ was seen when the crack width was between 0.05 and 0.10 in.

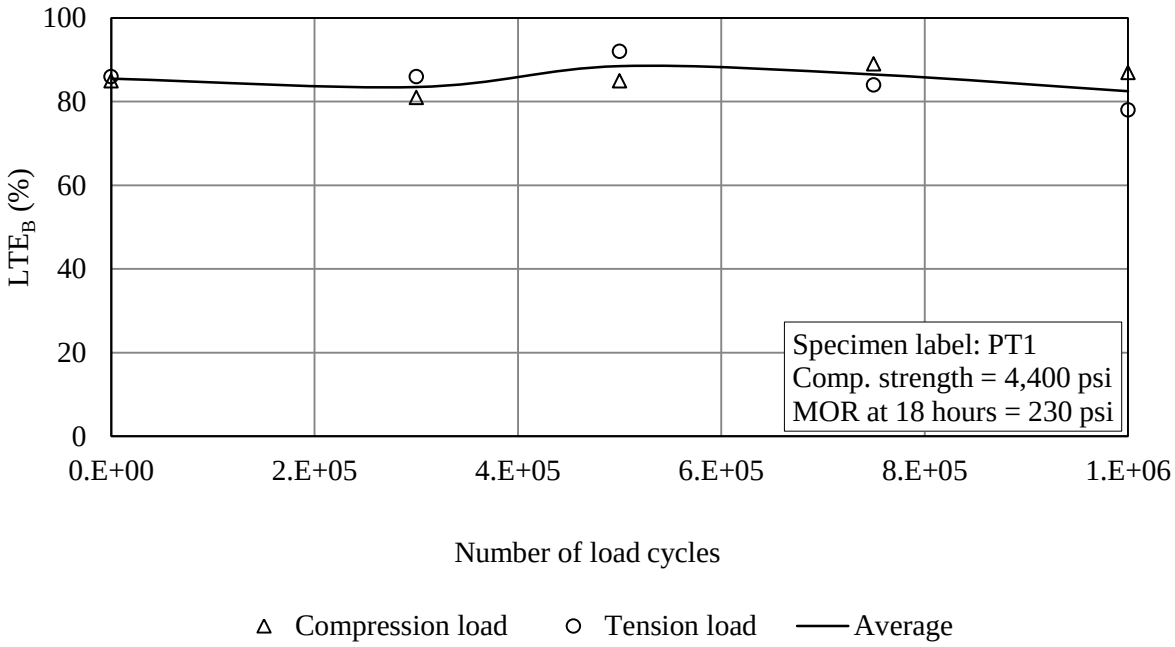

Figure 4-6: LTE vs number of load cycles for PC trial beam, PT1.

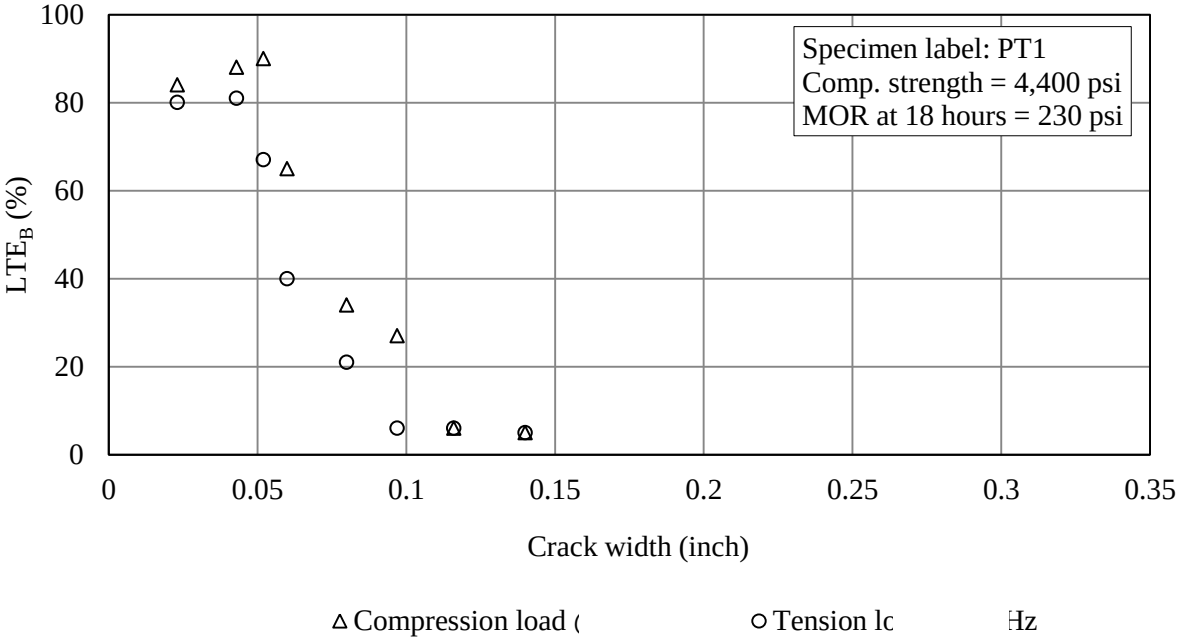

Figure 4-7: LTE vs crack width for PC trial beam, PT1.

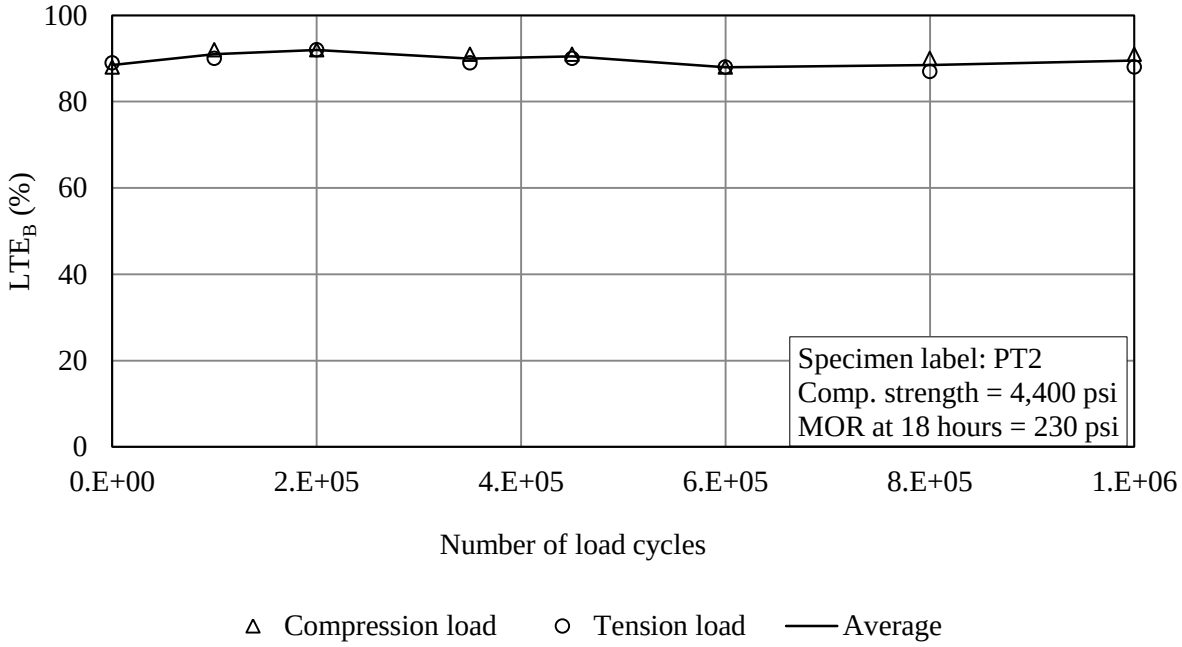

Figure 4-8: LTE vs number of load cycles for PC trial beam, PT2.

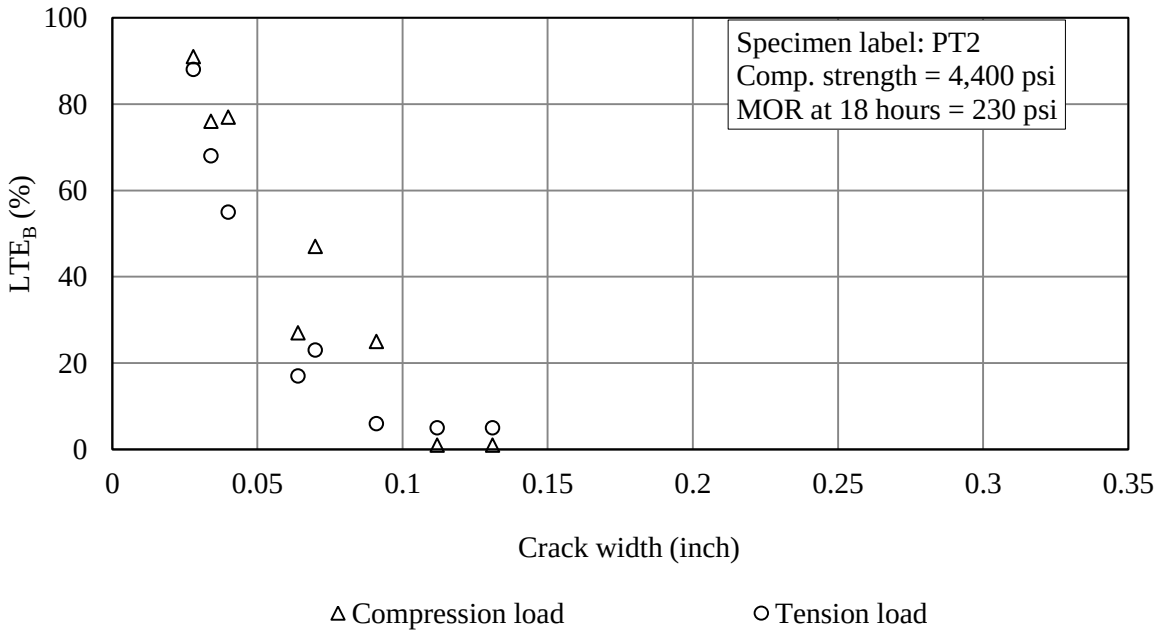

Figure 4-9: LTE vs crack width for PC trial beam, PT2.

The first reported FRC1 trial beam, F1T1 was fatigued at a 0.028-in crack width (Figure 4-10). It can be seen that the LTE_B decreased marginally (only by 1.5 percent) after 1 million load cycles. The difference between the $LTE_{B(t)}$ and $LTE_{B(c)}$ was negligible during the fatiguing. The interesting (and expected) observation was that the LTE_B did not sharply decrease when the crack width was increased, unlike with the PC beams.

The second reported FRC1 trial beam, F1T2, was fatigued at a considerably wider crack width, 0.05 inches. The average decrease in LTE_B was observed to be 6 percent. This beam was cast with a Type I cement. The compressive strength was only 1,500 psi at the time of testing time (7 days after casting). Probably because of the lower concrete strength, the LTE_B quite sharply decreased when the crack width was increased.

One of the common observations when testing all four beams was that the difference between the $LTE_{B(t)}$ and $LTE_{B(c)}$ was larger when the crack width was between 0.05 to 1.0 in. This difference was the result of macrotexture of the crack. Most of the time, the crack does not propagate completely vertical and perpendicular to the surface of the beam. This results in more engagement of the two fractured crack faces in one loading direction compared to the other, and thus LTE_B becomes higher in the former. When the crack width is narrow, the influence of the slope or the macrotexture of the crack face is low. At a lower crack width, the difference in the effective interlocking areas between two the directions is negligible. Again when the crack width is extremely large (> 0.1 in), the aggregate interlock engagement in both the directions substantially decreases; thus LTE_B becomes insensitive to the side of the crack that is loaded.

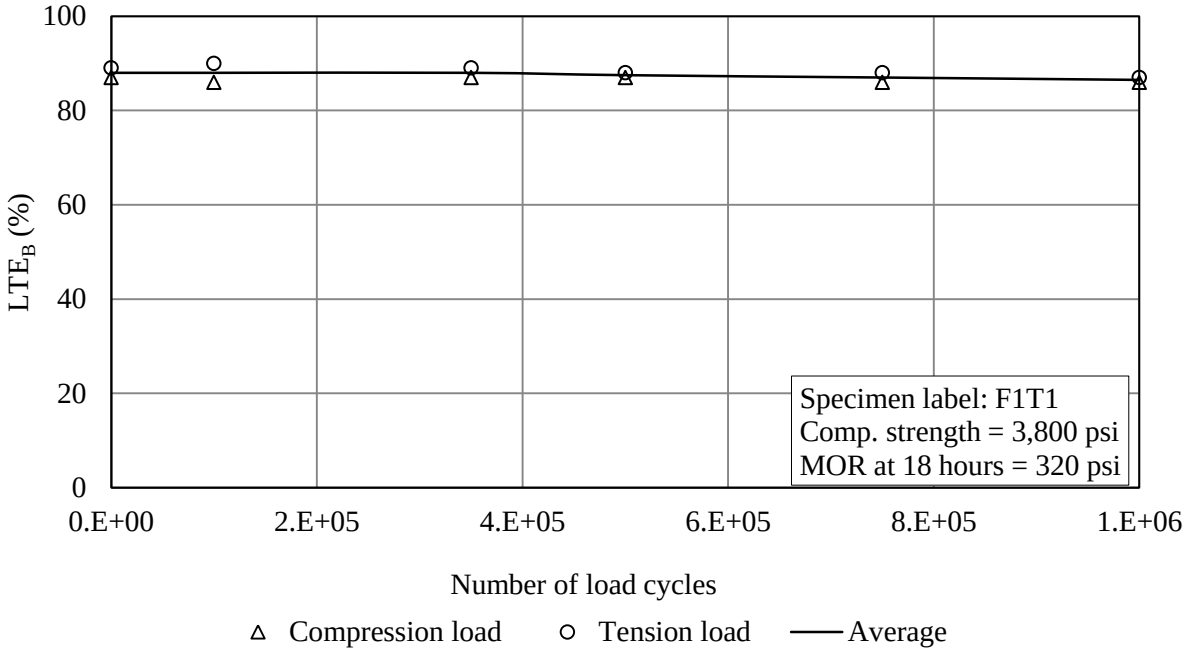

Figure 4-10: LTE vs number of load cycles for FRC1 trial beam, F1T1.

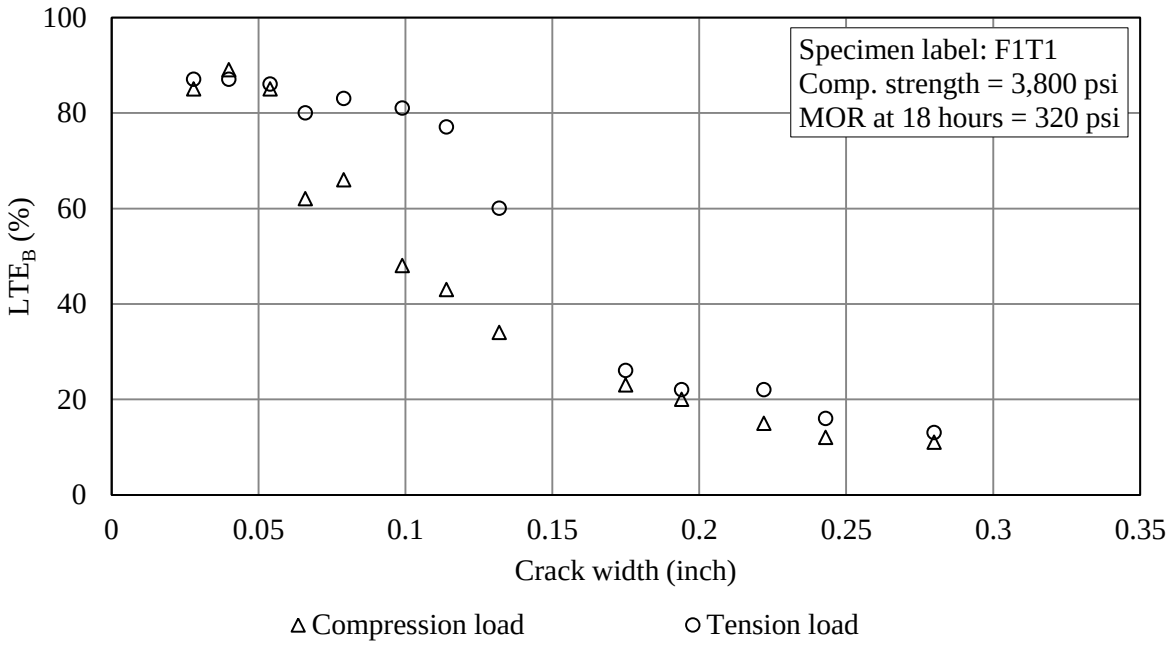

Figure 4-11: LTE vs crack width for FRC1 trial beam, F1T1.

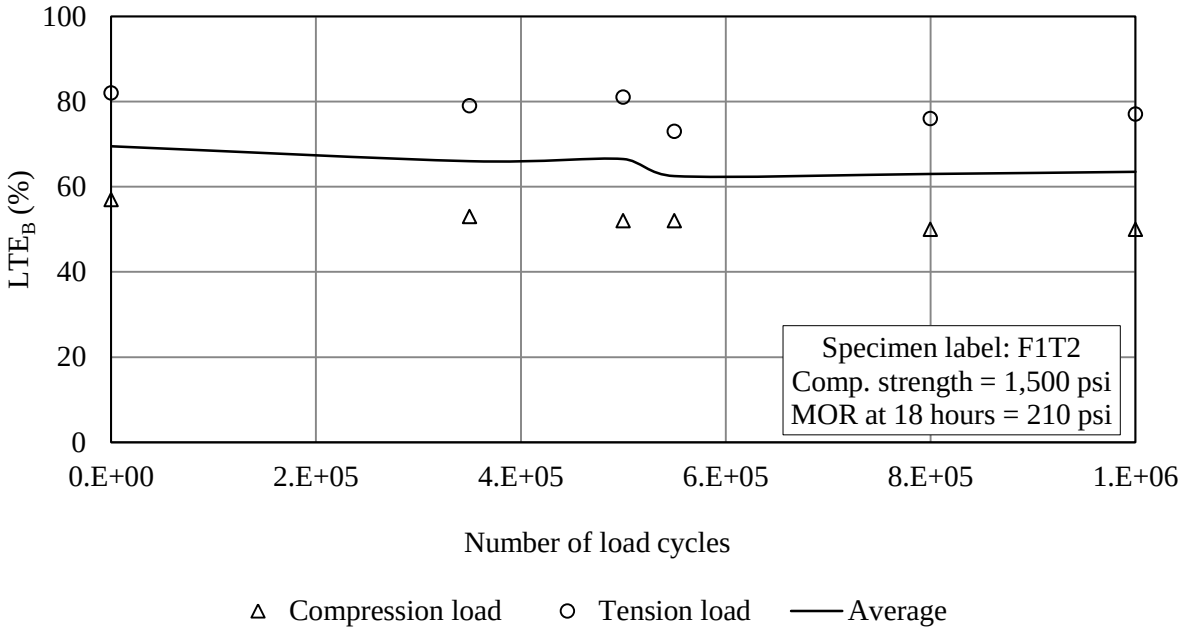

Figure 4-12: LTE vs number of load cycles for FRC1 trial beam, F1T2.

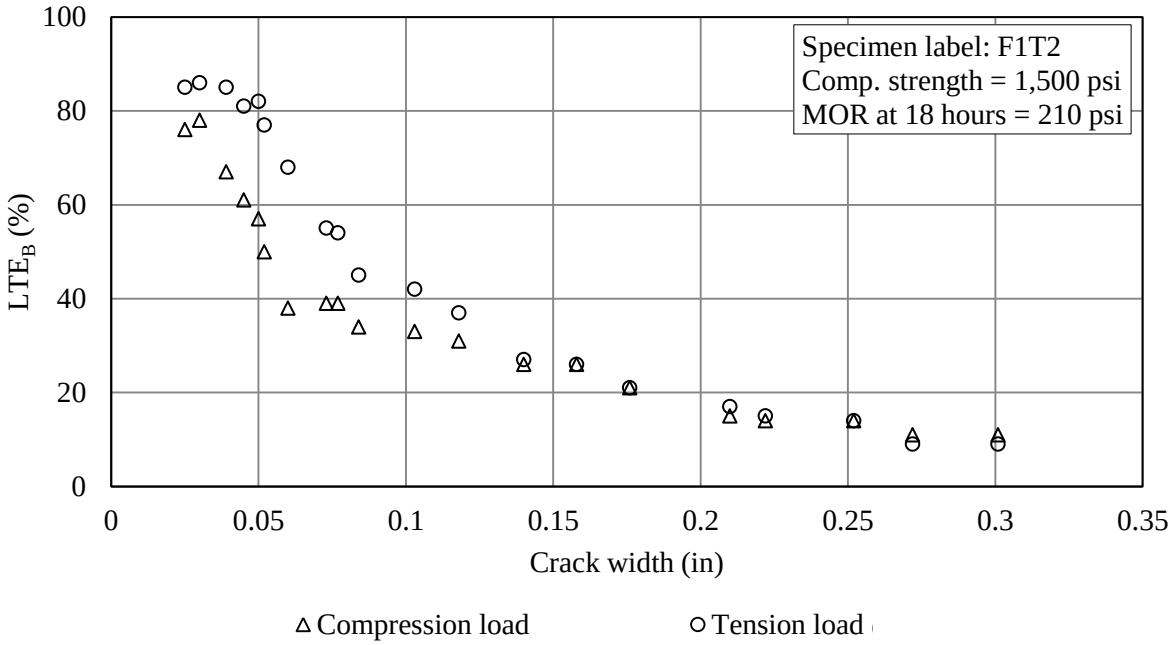

Figure 4-13: LTE vs crack width for FRC1 trial beam, F1T2.

A few beams were also tested at a very narrow crack width, such as 0.015 in. The problem associated with fatiguing at this crack width was the requirement of a higher horizontal

compression force to maintain such a tiny crack width, especially in the case of PC beams. This higher compression along the longitudinal axis compels the two halves of the beam to behave like a single unit. This deters any mechanical action, such as, sliding at the joint when loading. Both halves of the beam deflect with a single slope and do not rotate at the joint. The differential deflection thus becomes zero. In the case of FRC beams, although a horizontal compression force is not necessary, the fibers probably transfer moment across the crack width when the crack width is very narrow. Therefore a similar response was observed for narrower crack widths, such as 0.015 in.

On the basis of these observations, it was decided that the beams would be fatigued at crack widths larger than 0.015 in. At a 0.025-in crack width, the LTE_B in both PC and FRC beams is higher, whereas after a 0.060-in crack width, the LTE_B is quite lower. Therefore, it was decided that the actual test beams would be fatigued at two intermediate crack widths, 0.035 and 0.05 in. These two crack widths are also a good representation of the crack width range that the MnROAD whitetopping sections exhibited for a large period of the year (Chapter 2). Also as suggested by Jensen & Hansen, 2001, the aggregate interlock load transfer phenomenon plays a more significant role in this crack width range.

The complete test matrix for the B_{ALT} procedure is given in Table 4-7. Four beams for each concrete mixture were tested to derive the LTE_B vs N relationship. Two of them were fatigued at 0.035-in and the other two were fatigued at 0.05-in crack widths. These crack widths will be referred as the fatiguing crack width. In all four beams, before fatiguing, the crack width was incrementally increased from the initial existing crack width to the fatiguing crack width. At each increment, load and deflection profiles were recorded for five successive load cycles, after applying 995 seating loading cycles. At the fatiguing crack width, one million load cycles are

applied, except when a constant LTE_B was observed through a considerable range of cycles before reaching one million. For at least six consecutive load cycles, load and deflection profiles were recorded in the middle of the fatiguing process. The crack width was measured after every 50,000 load cycles to ensure a constant crack width was maintained. After fatiguing, the crack was again opened incrementally to record the load and deflection profiles at different crack widths. At each crack width, seating load cycles were again applied before recording the load and deflection profiles to ensure the system had stabilized.

The selection of one million as the number for load cycle applications was made based on the fact that most UTW projects are constructed for lower traffic volumes. Although one million load cycles do not represent the design life for all of the existing UTW projects, a large number of projects in the country develop distresses around one million ESALs (Barman, et al., 2010). Therefore, investigating the joint condition for up to one million load cycle repetitions can be considered appropriate amount for establishing a performance trend. Another consideration in making this choice for number of repetitions is the affordability of the resources and time for conducting each test. One beam was loaded to 10 million ESALs to establish the effects of fatigue on fiber performance. Apart from these above mentioned four beams, one separate beam was tested for each concrete mixture to evaluate the joint performance as a function of crack width when joints are not fatigued.

Table 4-7: Specimen matrix for B_{ALT} procedure.

Concrete category	Number of specimen	Fatiguing crack width
PC	2	0.035
	2	0.050
	1	Not fatigued
FRC1	2	0.035
	2	0.050
	1	Not fatigued

FRC2	2	0.035
	2	0.050
	1	Not fatigued

4.5 Test Plan for the S_{ALT} Procedure

The financially expensive component of the laboratory study was the casting and testing of the S_{ALT} specimens. Because of the financial and time constraints, only one slab for each concrete mixture was cast and tested. The fatiguing crack width in each concrete category was established baed on the the joint performance results obtained in the corresponding B_{ALT} procedure. The PC slab was fatigued at a 0.035-in crack width. Fatiguing of the FRC1 slab was started at a 0.035-in crack width. Unfortunately, this crack width did not remain constant during the fatiguing process. It increased to 0.049 in by the end of the fatiguing. The FRC2 slab was fatigued at a 0.050-in crack width. A more comprehensive discussion regarding the selection of the fatiguing crack width in the S_{ALT} procedure is provided after the presentation of the B_{ALT} test results, in the next chapter.

4.6 Conclusions

This chapter presented the properties of the materials used in this study. One plain concrete and two fiber reinforced concrete mixes were included. The mixture proportions for both the PC and FRC were similar, except that two separate types of fibers were added in the two FRC mixes. The test description for the B_{ALT} and S_{ALT} joint performance test is presented in this chapter. Results of a few B_{ALT} trial beams were also discussed to support the selection criteria of the fatiguing crack widths for the B_{ALT} testing to be performed.